RSC Advances

ROYAL SOCIETY OF CHEMISTRY

www.rsc.org/advances

Journal Name

ARTICLE

Branched Gold Nanoparticles on ZnO 3D Architecture as Biomedical SERS Sensors

Received 00th January 20xx,
Accepted 00th January 20xx

DOI: 10.1039/x0xx00000x

www.rsc.org/

S. Picciolini,[a] N. Castagnetti,[b] R. Vanna,[a] D. Mehn,[a] M. Bedoni,[a] F. Gramatica,[a] M. Villani,[b] D. Calestani,[b] M. Pavesi,[c] L. Lazzarini, [b] A. Zappettini*,[b] and C. Morasso*[a]

Surface-enhanced Raman Spectroscopy (SERS) widely improves the sensitivity of traditional Raman analysis, thus allowing this technique to be exploited for the development of new bio-analytical tests. In this work, 3D substrates made of zinc oxide tetrapods (ZnOTP) are decorated with branched gold nanoparticles by means of a new photochemical approach. The SERS enhancing properties of the obtained substrate are tested using different Raman dyes and apomorphine, a drug used for the management of Parkinson disease. The results prove that the enhancing properties depend on the shape of the gold nanoparticles grown on the branches of ZnO tetrapods. The optimized substrate here developed is characterized by an enhancing factor up to $7x10^6$ and a detection limit for apomorphine of 1 µM. Finally, the new substrates are tested to study single cancer cells showing enhanced Raman signals related to the portion of the cell interacting with the 3D structure of the substrate.

Introduction

The development of new bio-analytical tests, able to simultaneously provide a large number of data with high specificity and sensitivity, is becoming an important driving force of biomedical research especially in the general framework of "personalized medicine" where a precise stratification of patients is required to provide tailored therapies and treatments.[1,2] Surface enhanced Raman spectroscopy (SERS) is considered being a very promising tool for the development of new biomedical sensors. This technique couples the high number of data that can be obtained thanks to the well resolved Raman spectra, with a very good sensitivity achieved through the amplification of signals that is observed when the molecule of interest lies on, or is very close to, the surface of suitable plasmonic nanoparticles or nanostructured materials.[3] Despite the fact that the precise mechanism behind this enhancement is still to be completely understood, it is generally accepted that the main amplification factor is given by the so called "electromagnetic enhancement" related to the presence of regions on the substrate, characterized by a very intense electric field, named "hot spots".[4]

This great potential has driven the development of a number of different SERS substrates able to enhance Raman signals such as structures generated by e-beam lithography,[5] gold layers deposited on micropatterned surfaces,[6] assembly of silver nanorods deposited on closely packed silica nanospheres[7] and arrays of nanoholes or dielectric cavities embedded in a gold layer.[8,9] 3D SERS substrates are a particular group of substrates made of gold or silver nanoparticles supported on a complex non flat matrix. These substrates are appositely designed to increase the surface available in order to increase the number of hot spots thus obtaining an higher enhancement.[10,11] Within the possible supports that can be used for this aim, ZnO nanostructures are particularly appealing. They are characterized by an extreme surface to volume ratio, they do not absorb visible light, can be easily produced in high amounts with a good control on their shape and size and size and they are stable at air exposure.[12,13,14] Besides, several report in literature suggest how noble metal nanoparticles supported on ZnO are characterized by higher SERS enhancement factors.[15,16,17].
For all these reasons, in the last years, different groups have proposed highly active 3D SERS substrates made of gold or silver nanoparticles supported on zinc oxide nanostructures.[18,19,20,21]
One of the limitations to this approach, however, is that ZnO rapidly dissolves in acidic conditions, including in presence of tetrachloroauric acid ($HAuCl_4$) often used as precursor of gold nanoparticles. Therefore, in most studies, the decoration of the support with the noble metal nanostructures is performed

[a] *LABION - Laboratory of Nanomedicine and Clinical Biophotonics; Fondazione Don Carlo Gnocchi ONLUS, P.le Morandi 6, 20212, Milan, Italy.*
[b] *IMEM-CNR, Parco Area delle Scienze 37/A, 43124 Parma, Italy*
[c] *Parma University, Phys. Dept., Parco Area delle Scienze 7/A, 43124, Parma, Italy*

Electronic Supplementary Information (ESI) available: [details of any supplementary information available should be included here]. See DOI: 10.1039/x0xx00000x

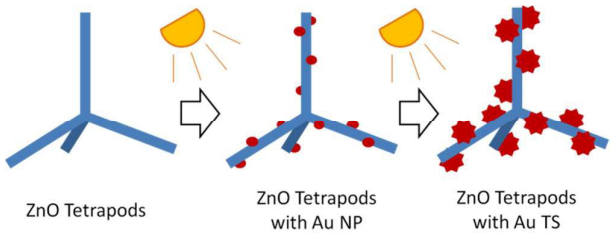

Figure 1. Schematic representation of the light assisted preparation of the SERS substrate made of ZnOTP decorated with branched gold nanoparticles.

either by thermal evaporation, which however does not allow the preparation of defined nanostructures on the surface, or by conjugating already preformed gold nanoparticles on the surface thanks to the use of linkers or surfactants, whose presence however could hinder the SERS efficacy.

In the present work, we describe a new and efficient 3D SERS substrate based on the use of ZnO tetrapods (ZnOTP) decorated with branched gold nanostructures nucleated and grown *in-situ* on ZnOTP surface specifically developed for being used in biomedical related applications.

The substrate has been prepared using a multi-step approach, briefly described in figure 1. First, spherical gold nanoparticles were synthesized by means of a photo reductive process on top of ZnOTP. Then, the obtained gold nanoparticles were used as seeds to prepare larger branched nanoparticles by means of a reduction process based on the use of HEPES buffer.

Among the different metal nanostructures proposed as SERS substrates branched noble metal nanoparticles are considered to be the most effective kind of nanoparticles because they are able to generate "hot spots" at the tips of their braches.[22,23] Supporting a large number of branched nanoparticles in a small volume is thence a promising approach for the preparation of a highly active, new SERS substrate. Besides, the proposed method is based on a photo-assisted reduction of the gold precursor, similarly to other works done using silver nanostructures,[24] without the use of surfactant or other capping agents that could contaminate the surface of the substrate.

The SERS enhancing properties of ZnOTP conjugated with spherical and branched gold nanoparticles have been tested using malachite green (MG) and rhodamine 6G (R6G); these are well-known dyes characterized by clearly recognizable Raman spectra. Besides, in order to prove the ability of the SERS substrate to detect a broad range of molecules, we have also studied its effectiveness in the detection of apomorphine, a dopamine agonist used for the management of symptoms in patients affected by Parkinson disease,[25] for which we observed a detection limit of 1 µM (0,27 µg/ml). Finally, in order to prove the potentialities of using this new SERS substrate for biological applications we evaluated the properties of ZnOTP decorated with branched nanoparticles for the SERS analysis of single cancer cells.

Experimental

Materials and methods

All chemicals were purchased from Sigma–Aldrich (St. Louis, MO) and used as received. Water was deionized and ultra-filtered by a Purite Select Fusion apparatus from Purite (Oxfordshire, UK).

Synthesis

Preparation of ZnOTP: ZnOTP were prepared according to a previously published method described in ref. [26] and [27].

Preparation of gold seeds on ZnOTP: 10 mg of ZnOTP were dispersed in 50 ml of isopropyl alcohol by sonication. The suspension was stirred at room temperature, illuminated with a 300 W halogen lamp and 100 µL of 1 mM aqueous solution of $HAuCl_4$ were added every 10 minutes for 2 hours. Nanostructures were then washed with deionized water, deposited onto a 3x3 mm silicon chip by centrifugation, and dried in an oven at 110°C for 1h under vacuum (10^{-2} mbar).

Preparation of branched gold nanoparticles on ZnOTP: The previously obtained substrate supporting spherical gold seeds on ZnOTP was immersed in 2.5 mL of a 5 mM aqueous solution of 2-[4-(2-hydroxyethyl)-1-piperazinyl]ethane-sulfonic acid (HEPES) at pH 7.3. After dipping the chip in HEPES, 0.5 mL of $HAuCl_4$ (0.8 mM) was slowly added drop by drop. The chip was then kept at room temperature and under light exposure for 30 minutes followed by washing steps in water (three times).

Spectroscopy

Absorption spectroscopy: The optical absorption spectra were measured on samples at room temperature by using a Varian 2390 spectrophotometer equipped with a diffuse reflectance sphere.

FE-SEM analysis: Sample morphology was investigated using a Zeiss Auriga Compact Field Emission Scanning Electron Microscope with accelerating voltage ranging in 5-15 kV.

SERS experiments on small molecules: Raman spectra were recorded using an Aramis Raman microscope from Horiba Jobin-Yvon equipped with a He-Ne laser light source operating at 633 nm and a 50x objective. DuoScan acquisition mode was used in order to increase reproducibility. Typically a 0.40 µL drop of each analyte solution was dropped on the chip and dried at room temperature. Afterwards Raman spectra were collected from multiple positions randomly selected on the surface. For the measurement of malachite green, rhodamine 6G and apomorphine 5 mW of source power was utilized with an acquisition time between 1 and 5 seconds.

SERS experiments on cells: HL-60 cells (acute leukemia cells) were cultured in RPMI-1640 medium supplemented with 20% fetal bovine serum, 1% PenStrep and 1% L-Glu. Around $1x10^6$ cells were washed twice with PBS by centrifugation (400g for 8 min), fixed with 2% formaldehyde (37 °C for 15 minutes), washed three times with PBS at RT and resuspended in the same buffer to reach a final concentration of $1x10^6$ cell/ml. For the experiment a layer of ZnOTP decorated with gold nanospheres was deposited on a quartz slide and then treated as described above for the production of the branched

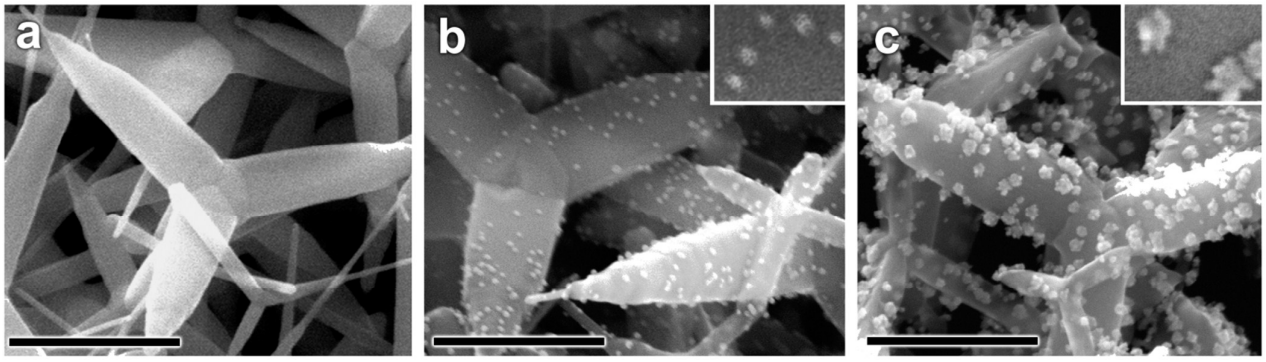

Figure 2:. a) FE-SEM images of as-grown ZnOTP; b) ZnOTP after photochemical functionalization with gold spherical nanoparticles; c) ZnOTP after seed-mediated growth of branched nanoparticles. Scale bar = 300 nm in all samples

particles. This SERS substrate was then placed in a petri dish and immersed in PBS. An aliquot of 200 µl of cell suspension was directly deposited in the middle of the disc. After 10 min of cell sedimentation the SERS experiment was performed by using an immersion objective (63x/1.0 NA, W-Plan-Apochromat, Carl Zeiss, Jena, Germany) and the Raman system described above. For these experiments 10 mW of source power was utilized with an acquisition time of 2 seconds and a laser spot size of about 1.5 µm. The cell was then analyzed by scanning the entire cell with a step size of 0.8 µm in order to select the most representative SERS spectra."

Typical Raman measurements were performed by using an identical procedure and identical acquisition parameters except for using a CaF_2 instead of the SERS substrate.

Results and discussion

Preparation of SERS substrate

The SERS substrate was obtained through a three steps process depicted in Figure 1. First, ZnOTP (Fig. 2a) have been grown from vapour phase with a very large yield, starting from 5N Zn powders only, without any precursor or catalyst. A continuous reaction/oxidation process with O_2 in a tubular furnaces allowed a multi-gram scale synthesis in a laboratory reactor at 700°C, as previously reported.[28,29]

The second step (Fig. 2b) consisted in the synthesis of spherical gold seeds by photo-reduction. As-grown ZnOTP were dispersed in the solvent of choice (e.g. isopropyl alcohol) containing a predetermined amount of gold precursor ($HAuCl_4$) and applying sonication and mechanical stirring.

The mixture was illuminated by a halogen lamp to promote the formation of electron hole-pairs inside the ZnO: photo-generated carriers are the driving force for the redox process. Indeed the UV radiation promotes near band edge transition inside ZnO nanostructures: on one hand, conduction band electrons reduces Au(III) to Au(0) at the semiconductor surface, resulting in the nucleation/growth of Au(0) nanoparticles. On the other hand, valence band holes oxidize isopropyl alcohol to acetone in order to retain electro-neutrality. Upon variation of gold precursor content and illumination time, different Au nanoparticles dimensions and density have been obtained (Figure S1 in Supp. Inf.) influencing the following nucleation of Au branched nanoparticles. Such photochemical approach allowed the production of gold seeds characterized by uniform dimension directly on the surface of the tetrapods and without the need of any organic linker or surfactant that could hinder the SERS enhancing properties of the substrate itself. The obtained gold-functionalized ZnOTP were then deposited on silicon substrates by centrifugation. In the third step (Fig. 2c) the solid SERS substrate was prepared by the seed-mediated growth of branched gold nanoparticles on top of ZnTP. The growth has been performed by adding $HAuCl_4$ in presence of HEPES, a buffer used in biological laboratories, here used as reducing agent as previously described by Xie and co-workers.[30]

In the present work, HEPES buffer also acts as shape directing agent[30] and is necessary to keep the pH at a neutral value to protect ZnOTP from the dissolution that other ways would occur in presence of the relatively high concentration of tetrachloroauric acid used.

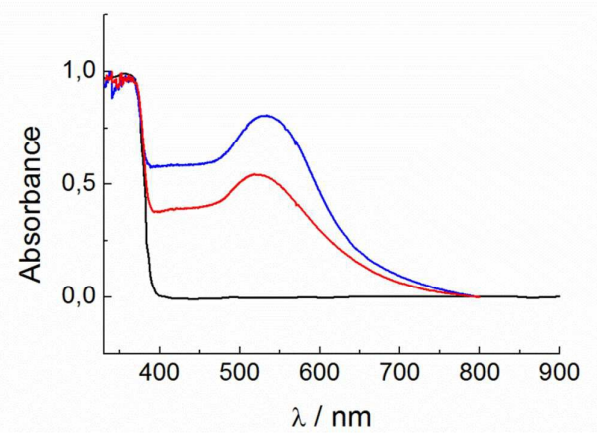

Figure 3: Absorption spectroscopy, from bottom to top, of ZnOTP (black), ZnOTP decorated with spherical nanoparticles (red) and ZnOTP decorated with branched particles (blue).

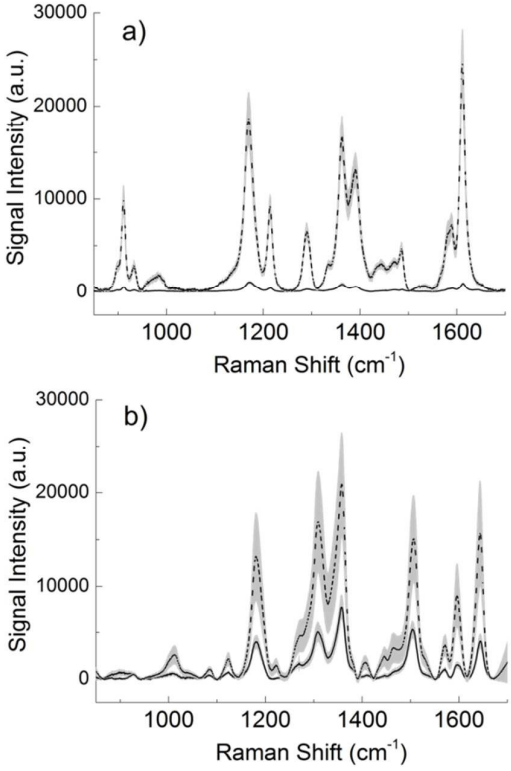

Figure 4: SERS spectra of MG 10 µM (a) and R6G 100 µM (b) acquired under the same conditions using ZnOTP decorated spherical (full) and branched (dashed) gold nanoparticles (standard deviation of the signal is given by the grey shadow and is 15% for the peak at 1611 cm^{-1} of MG and 25% for the peak at 1358 cm^{-1} of R6G). Spectra have been acquired using a 5 mW HeNe laser operating at 633 nm focused on the surface with a 50x objective and applying 1 second of accumulation time for MG and 5 second of accumulation time for R6G.

FE-SEM analysis (Fig. 2b-c) and UV-Vis absorption spectroscopy (Fig. 3) confirmed the presence of the gold seeds first and of the branched nanoparticles on the surface of the ZnOTP after the HEPES treatment. This morphological investigation reveals an homogenous distribution of gold seeds with a diameter of about 7-8 nm on the surface of ZnOTP without any detectable sign of aggregation and, as a consequence, an homogeneous distribution of the branched particles having an average diameter of ≈ 20 nm and arms of about 5-8 nm (See STEM images in Figure S2 Supp. Inf.). According to the SEM investigation, this process is highly efficient as the nucleation process clearly takes place starting from the previously obtained seeds as proved by the fact that only a small fraction of seeds remains on the surface and that the density of gold seed nanoparticles per area unit is consistent with that of branched gold nanoparticles.

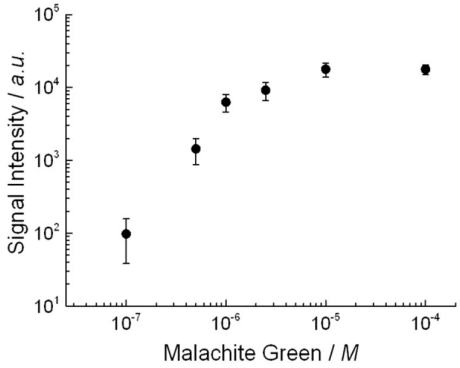

Figure 5: Intensity of SERS spectra of MG (measured at 1170 cm^{-1}) obtained at different concentrations. Full spectra obtained at each concentration can be found in Figure S5 of the supplementary information.

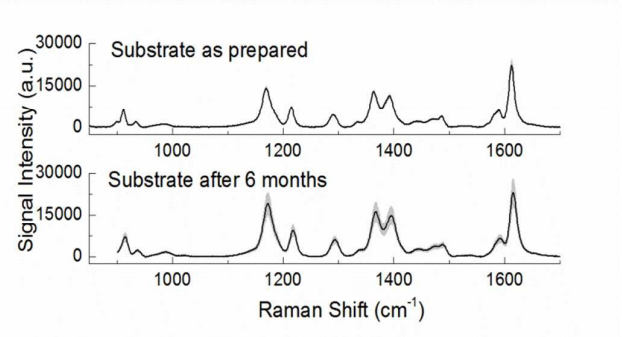

Figure 6: Intensity of SERS spectra of MG 100 µM measured on a substrate immediately its preparation (Top) and after 6 months at air exposure (bottom)

At the same time HEPES molecules do not stay on the surface of the substrate as proved by the Raman spectra shown in Figure S3.

The decoration of ZnOTP with gold nanostructures extends the light absorption of the coupled nanostructure into the visible range (Fig. 3). The absorption maximum corresponds to the localized surface plasmon (LPR) of nanosized gold (about 2.4 eV) and it is higher for the branched gold nanoparticles: this can be ascribed either to the overall larger dimensions of the branched nanoparticles and to the higher content of gold compared to the case of spherical nanoparticles. Besides, a red shift of the absorption threshold is visible in the case of the branched nanoparticles. This effect is addressed to the shape anisotropy of Au: the braking of spherical symmetry splits the LPR absorption peak creating a lower energy mode that broadens towards lower energy. On the other hand, the limited shift of the plasmonic peak confirms that the obtained branched nanoparticles remain isolated and do not aggregate. This clearly indicates that the higher SERS enhancing properties of the substrate after the HEPES treatment must be ascribed to the particular shape of the gold nanoparticles and not to the formation of aggregates.

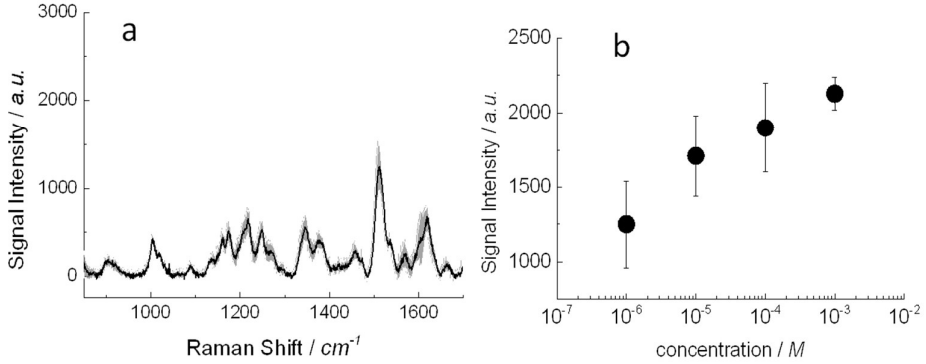

Figure 7: a) SERS spectrum of apomorphine acquired at 1 µM. Full line represents the average of 9 spectra obtained inside an area of 50 x 50 µm on the substrate; grey shadow represents the standard deviation. b) concentration dependence of the signal (intensity of the peak at 1511 cm^{-1}) observed using apomorphine at different concentrations. Full spectra obtained at each concentration can be found in Figure S6 of the supplementary information.

The absorption plateau above 2.4 eV is due to gold interband transition involving *d* and *sp* orbitals [31] while the near band edge ZnO absorption is visible at 3.2 eV [32].

Characterization of the SERS enhancing properties

The enhancing properties of ZnOTP decorated with spherical and branched gold nanoparticles have been tested measuring MG and R6G using a 633 nm excitation laser line. Therefore, MG was measured in resonance with its absorption band centred at 617 nm, while R6G was measured in non-resonant conditions having an absorption band centred at 526 nm. See UV-Vis absorption spectra in Figure S4 in Supp. Inform.

The results of this study are summarized in Figure 4 and clearly show that, as expected, ZnOTP samples coated with Au branched nanoparticles are more effective than the corresponding ones coated with spherical nanoparticles.

The limit of detection and the linearity of the optimized SERS substrate have been determined drying small drops of MG at different concentrations on top of the substrate made of ZnOTP decorated with branched nanoparticles and acquiring Raman spectra from 100 different positions distant from the border of the drop to avoid the variability given by the coffee ring effect (see Figure S5 in the Supp. Inform. the spectra acquired at 1 µM concentration as example). Figure 5 shows the intensity of the peak at 1170 cm^{-1} of the MG SERS spectra, corresponding to the in-plane mode of the aromatic C-H bending, obtained using different concentrations of the dye. The limit of detection has been determined to be 100 nM and a linear increment of the signal intensity was observed up to 1 µM where a progressive saturation of the signal occurs suggesting a rather high affinity of the dye for the area of the substrate where the "hot spots" are located. A rigorous calculation of the enhancement factor provided by the substrate is difficult to obtain as the exact number of "hot spots"; the variation given by small differences in the nanometric features of each branch and the exact number of molecules effectively contributing to the signal are not known. However the analytical enhancing factor (EF) reflecting the average situation can be obtained according to the simple Equation 1:

$$EF = (I_{SERS} / I_{Raman}) * (M_{Raman} / M_{SERS}) \quad (1)$$

where I_{SERS} and I_{Raman} are the peak intensities observed using the substrate and a simple silicon wafer respectively. M_{SERS} is the concentration of the dye solution used for SERS experiment and M_{Raman} is the concentration in the solution applied on silicon. According to the data collected, we obtain a robust EF of about $7x10^6$ for samples decorated with branched Au nanoparticles and of $2x\ 10^5$ for the samples decorated with the spherical seeds.

At last we studied the long term stability of the substrate. Both ZnOTP and Au based nanomaterials are known for being very stable at air exposition as they do not suffer of oxidation related degradation. The SERS enhancing properties of a ZnOTP substrate decorated with branched gold nanoparticles have been tested immediately after preparation and after six month at air exposition and room temperature. As shown in figure 6 the intensity of MG SERS spectra remains very similar confirming the efficacy of the substrate even after a long exposure to air.

SERS detection of Apomorphine

In order to study the efficiency of the developed substrate, we tested the system for the detection of apomorphine, one of the most used drugs for the management of the symptoms of Parkinson disease that is administered by subcutaneous injection. It is well known that apomorphine, despite being effective in providing a reduction of tremors and allowing a partial rehabilitation of motor skills,[33] is not equally active on all patients[25] and, in particular, its metabolism rates may vary among patients, thus resulting in different plasma levels observed in each patient.

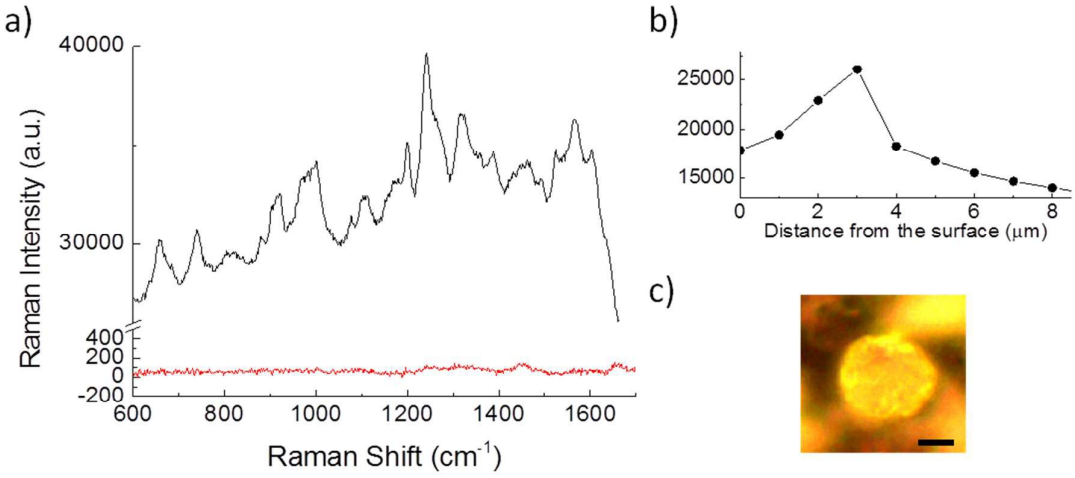

Figure 8: a) SERS spectrum of a single HL-60 cell deposited on branched gold nanoparticles decorated ZnOTP (black) compared with the Raman signal of a HL-60 cell deposited on CaF2 (red). b) average SERS signal, calculated in the region between 1400-1700 cm-1, measured at different distances from the slide surface. c) HL-60 cell positioned on the SERS substrate and observed in bright-field. The SERS and Raman spectra in the plot, the SERS signal distribution and the bright-field images were acquired at 3 μm above the slide surface. The Raman and SERS spectra are plotted with a different scale for clarity.

This example underline the need of the development of new methods for a rapid assessment of drug plasma concentration that could facilitate therapy monitoring and therefore more personalized treatments of infections and chronic diseases treated with drugs with a small therapeutic window.[34] Despite the sensitivity of SERS is still not equal to the one of other separation based techniques such as HPLC-MS, the minimal sample preparation together with the relatively cheap instrumentation used in SERS analysis would make this approach a promising route for the therapeutic monitoring of drugs.

In a previous study, we demonstrated how it is possible to detect apomorphine by mean of SERS using branched gold nanoparticles in suspension.[35] Here we decided to test the hypothesis that supporting a large number of these nanoparticles in a smaller volume by means of a 3D network could be useful to increase the efficacy of this approach. As shown in Figure 7, we have been able to detect the drug at 1 μM, a concentration 5 times lower than the one achieved in solution with a good concentration dependence of the signal up to 1 mM (Figure 7b).

The spectrum reported in Figure 6a is characterized by the presence of three well resolved peaks in the region of 1520–1620 cm^{-1} that are ascribed to the C=C stretching of the two aromatic rings; in addition, the peaks at 1004 cm^{-1} and 1217 cm^{-1} correspond to vibrations of the aromatic rings and to the aromatic CH in-plane bending, respectively.

Interesting, the SERS spectrum is characterized by the presence of some bands related to the oxidation of apomorphine that could happen on the surface of our particular metal substrate.

For example, the strong peak at 1374 cm^{-1}, that is not present in the standard Raman spectra of apomorphine (Figure S8 in Supp. Inform.), is related to the CO stretching and the aromatic CH in-plane bending and suggests that the molecule is present in its oxidized form. To confirm this, the peak at 1300 cm^{-1} in the Raman spectrum, which corresponds to OH in-plane bending mode, is lost in SERS spectrum, because the OH groups are oxidized to C=O bonds. This result is consistent with what previously reported in literature on the SERS analysis of apomorphine [35,36,37] and confirmed its effective detection.

Single cell SERS experiments

The SERS properties of ZnOTP substrates decorated with the branched nanoparticles were tested on single cells. HL-60 cells, which are cultured leukemia cells and granulocyte precursors, were used as models of circulating tumour cells. Figure 7 shows the results of the analysis of HL-60 cells deposited on the substrate. The strong enhancement of the Raman signal is clearly demonstrated by the comparison between the SERS spectrum and the Raman spectrum collected from HL-60 cells on a SERS inactive substrate (CaF_2). In addition, we verified that the SERS enhancement is related to the interaction between the SERS substrate and the cell. In fact, the signal intensity reaches the maximum at around 3 μm from the slide surface (Figure 8b), which corresponds to the interface between the cell and the top of the ZnO layer, and decreases rapidly when the laser is focused on the cell but at longer distances.

The HL-60 SERS spectra reveal some Raman features typical of cells: for example the signal around 1002 cm^{-1} assigned to proteins (phenylalanine) and the signal around 1451 correspondent to the CH_2 bending of proteins and lipids. In addition, other intense peaks identified here are not those

typically described in Raman studies of cells but they are related to the SERS effects (peaks assignation in Table 1).

As already described in other SERS studies,[38,39] the peaks observed here are most probably derived by the enhancement of a fraction of molecules positioned in close proximity (around 10 nm) to the SERS substrate. This is also confirmed by the peaks assignations which are mostly related to lipids and proteins.

Raman Shift [cm^{-1}]	Assignment[(a)]
656	C-S
732	C-S, Phosphatidylserine
919	C-C, proline/hydroxyproline
1002	C-C, phenylalanine
1106	C-C, carbohydrates
1200	Aromatic C-O and C-N
1245	Amide III
1315	CH_3, CH_2, lipids
1388	CH_3, lipids
1451	CH_3, CH_2, proteins, lipids
1566	COO^-
1602	C-C, phenylalanine

(a) Assignment has been obtained according to ref. [38] and [39]

Table 1: Assignment of SERS peaks of HL60 cells spectra.

Conclusions

In order to allow SERS to become an important tool for the biochemical studies there is still the need for an effective and reliable SERS substrate, which can be used fo enhance signal from a broad range of samples. This paper has provided one way to respond to these need by supporting on a 3D network of zinc oxide tetrapods (ZnoTP) an high number of branched gold nanoparticles. This approach allows to obtain an active solid substrate with a great amount of "hot spots", without the need to produce very narrow gaps between the noble metal nanoparticles that would limit the dimensions of the molecules to bestudied by means of SERS. In addition, the use of a surfactant free photochemical approach for the direct growth of small gold nanoparticles on the surface of ZnOTP allows the generation of well isolated spherical nanoparticles. that can be used as seeds for the subsequent preparation of the more SERS active branched nanoparticles.

By this doing we developed and optimized a simple protocol for the production of a new SERS substrate that couples the advantage of having highly SERS-active nanoparticles densely distrubuted in a 3D volume, thus increasing in turn the enhancing factor, togheter with the practical advantage related to the use of a solid SERS substrate, if compared with nanoparticles in solution.

The obtained SERS substrate material is characterized by good enhancing properties with a calculated analytical enhancing factor closed to 10^7, depending on the molecule observed, and has demonstrated to be active for the detection of a broad range of molecules interesting for biomedical applications such as Raman dyes (that can be used to specifically label biological targets) and drugs. Besides, as a proof of concept, we tested the possibility to use this material for the characterization of HL-60 cultured cancer cells demonstrating a noteworthy enhancement of the signal thus suggesting that this approach could become useful for the identification of particular cellular subtypes as well as for the study the cellular surface by SERS 3D solid substrates

Acknowledgements

Funding for this research was provided by Fondazione Cariplo (International Recruitment Call 2011 Project: An innovative, nanostructured biosensor for early diagnosis and minimal residual disease assessment of cancer, using surface-enhanced Raman spectroscopy) and by the Italian Ministry of Health (Conto Capitale 2010: Realizzazione e validazione di una core facility di biofotonica clinica per diagnosi precoce e monitoraggio di minimal residual disease in patologie tumorali).

Notes and references

*CM: Phone: +39-0240308533. Twitter: @CarloLabion E-mail: cmorasso@dongnocchi.it Website: http://www.labion.eu

* AZ: Phone: + 39-0521-269296. E-mail zapp@imem.cnr.it Website: http://www.imem.cnr.it/signal/

1 S. Carrara, S. Ghoreishizadeh, J. Olivo, I. Taurino, C. Baj-Rossi, A. Cavallini, M. Op de Beeck, C. Dehollain, W. Burleson, F. G. Moussy, A. Guiseppi-Elie, G. De Micheli, *Sensor* 2012, **12**, 11013-11060.

2 P. D. Howes, R. Chandrawati, M. M. Stevens, *Science* 2014, **346**, 1247390.

3 Y. Wang, J. Irudayaraj, *Phil Trans R Soc B* 2013, **368**, 20120026.

4 S. Schlücker, *Angew. Chem. Int. Ed.* 2014, **53**, 4756–4795.

5 G. Das, M. Chirumamilla, A. Toma, A.; Gopalakrishnan, R. Proietti Zaccaria, A. Alabastri, M. Leoncini, E. Di Fabrizio, *Sci. Report* 2013, **3**, 1792

6 N. M. B. Perney, J. J. Baumberg, M. E. Zoorob, M. D. B. Charlton, S. Mahnkopf, C. M. Netti, *Opt. Express* 2006, **14**, 847–857.

7 N. G. Greeneltch, M. G. Blaber, G. C. Schatz, R. P. Van Duyne, *J. Phys. Chem. C* 2013, **117**, 2554–2558.

8 A. G. Brolo, E. Arctander, R. Gordon, B. Leathem, K. L. Kavanagh, *Nano Lett.* 2004, **4**, 2015-2018.

9 S. Picciolini, D. Mehn, C. Morasso, R. Vanna, M. Bedoni, P. Pellacani, G. Marchesini, A. Valsesia, D. Prosperi, C. Tresoldi, F. Ciceri, F.; Gramatica, *ACS Nano* 2014, **8**, 10496–10506.

10 G. Wang, G. Y. Shi, H. Z. Wang, Q. H. Zhang, Y. G. Li, *Adv. Funct. Mater.* 2014, **24**, 1017-1026.

11 D. Mehn, C. Morasso, R. Vanna, M: Bedoni, D. Prosperi, F. Gramatica, *Vibr. Spect.* 2013, **68**, 45–50.

12 M. Zha, D. Calestani, A. Zappettini, R. Mosca, M. Mazzera, L. Lazzarini, L.; Zanotti, *Nanotechnology* **2008**, *19*, 325603.

13 D. Calestani, M. Zha, R. Mosca, A. Zappettini, M. C. Carotta, V. Di Natale, L. Zanotti,. *Sens. Actuator B-Chem* 2010, **144**, 472-478.

14 D. Calestani, M. Zha, L. Zanotti, M. Villani, A. Zappettini, *CrystEngComm* **2011**, *13*, 1707-1712.

15 S. Siddhanta, V. Thakur, C. Narayana, S. M. *ACS Appl. Mater. Interfaces* **2012**, 11, 5807-5812
16 T. Wang, Z. Zhang, F. Liao, Q. Cai, Y. Li, S.-T. Lee, M. Shao *Sci Report* **2014**, 4, 4052
17 K. Sivashanmugan, J.-D. Liaoa, B. H. Liua, C.-K. Yaoa, S.-C. Luo *Sensor Act. B* **2015**, 207, 430-436.
18 Y. Xie, S. Yang, Z. Mao, P. Li, C. Zhao, Z. Cohick, P. H. Huang, T. J. Huang, *ACS Nano* 2014, **8**, 12175–12184.
19 G. Sinha, L. E. Depero, I. Alessandri, *ACS Appl. Mater. Interfaces*, 2011, **3**, 2557–2563.
20 J. Huang, F. Chen, Q. Zhang, Y. H. Zhan, D. Ma, K. Xu, Y. X. Zhao, *ACS Appl. Mater. Interfaces* 2015, **7**, 5725−5735
21 H. Tang, G. Meng, Q. Huang, Z. Zhang, Z. Huang, C. Zhu .*Adv. Funct. Mater*. 2012, **22**, 218–224
22 L. Rodríguez-Lorenzo, R. A. Álvarez-Puebla, F. J. Garcia de Abajo, L. M. Liz-Marzán, *Phys. Chem. C* 2010**, 114**, 7336-7340.
23 A. M. Fales,H. Yuan, T: Vo-Dinh, *Langmuir* 2011, **27**, 12186-12190.
24 B. Nie, Q. Zhou, W. Fu, RSC Advances, 2015, 5, 24210-24214.
25 F. Stocchi, *Neurol. Sci*. 2008 **29**, 5:S383-6
26 W. R. Premasiri, D. T. Moir, M. S. Klempner, N. Krieger, J. II, L. D: Ziegler *J. Phys. Chem. B*, 2005, **109**, 312–320.
27 A. Sujith, T. Itoh, H. Abe, K. Yoshida, M. S. Kiran, V. Biju, M. Ishikawa, M. *Anal. Bioanal. Chem*. 2009, **394**, 1803-1809.
28 M. Villani, D: Calestani, L. Lazzarini, L.; Zanotti, R. Mosca, A. Zappettini, *J. Mater. Chem.*, 2012, **22**, 5634 – 5699.
29 L. Zanotti, D. Calestani, M. Villani, M. Zha, A. Zappettini, C. Paorici *Cryst. Res. Technol.*, 2010, **45**, 667–671.
30 J. Xie, J. Yang Lee, D. I. C. Wang, *Chem. Mater*. 2007, **19**, 2823-2830.
31 M. Aeschlimann, Electron Dynamics in Metallic Nanoparticles in *Encycl. Nanosci. Nanotechnol.*, (Ed. H. S. Nalwa) American Scientific Publishers 2004
32 Ü.Özgür, Y. I. Alivov, C. Liu, A. Teke, M. A.; Reshchikov, S. Doğan, V. Avrutin, S.-J. Cho, H. Morkoç, *J. Appl. Phys.* 2005, **98**, 041301.
33 A. Antonini, E. Tolosa, *Expert Rev Neurother.* 2009**, 9**, 859-867.
34 J. W. Ndieyira, N. Kappeler, S. Logan, M. A. Cooper, C. Abell, R. A. McKendry, G. Aeppli, *Nat. Nanotech*. 2014, **9**, 225–232.
35 C. Morasso, D. Mehn, R. Vanna, M. Bedoni, E. Forvi, M. Colombo, D. Prosperi, F: Gramatica, *Mat. Chem. Phys*. 2014 **143**, 1215-1221.
36 N. R. Agrawal, E. Fazio, F. Neri, S. Trusso, C. Castiglioni, A. Lucotti, N. Santo, P. M. Ossi *Cryst. Res. Technol.*, 2011, **46**, 836–840
37 A. Lucotti, M. Tommasini, M. Casella, A. Morganti, F Gramatica, G. Zerbi *Vibr. Spect.* 2012, 62, 286-291.
38 Z. Movasaghi, S. Rehman, I. U. Rehman, *Appl. Spectrosc. Rev.* 2007, **42**, 493-541.
39 J. De Gelder, K. De Gussem, P. Vandenabeele, L. Moens, L. *J. Raman Spectrosc.* 2007, **38**, 1133–1147.

